

Microwave imaging of piecewise constant objects in a 2D-TE configuration

O. Féron*, B. Duchêne and A. Mohammad-Djafari

*Laboratoire des signaux et systèmes (CNRS – Supélec – Université Paris-Sud 11), Plateau de Moulon,
3 rue Joliot Curie, 91192 Gif-sur-Yvette, France*

Abstract. In this paper we propose a stochastic algorithm applied to an electromagnetic inverse scattering problem. The objective is to characterise an unknown object from measurements of the scattered fields at different frequencies and for several illuminations.

This inverse problem is known to be nonlinear and ill-posed. It then needs to be regularized by introducing prior information. The particular prior information we account for is that the object is composed of a known finite number of different materials distributed in compact regions. The algorithm is applied to the inversion of experimental data collected at the Institut Fresnel (Marseille) and has already provided satisfactory results in a 2D-TM configuration. Herein, the goal is to test the same kind of method in a 2D-TE configuration.

Keywords: Microwave imaging, Bayesian estimation, Markov random fields

1. Direct model

We deal herein with an electromagnetic inverse obstacle scattering problem where the goal is to characterise unknown targets from measurements of the scattered fields that result from their interactions with a known interrogating (or incident) wave in the microwave frequency range. The configuration considered herein is that of the Institut Fresnel experiment [1]: an incident time-harmonic wave at angular frequency ω (the time-dependence $\exp(-i\omega t)$ is implied) illuminates a cylindrical target (considered as infinite along the \vec{Oz} axis and of arbitrary cross-section shape Ω in the (x, y) plane) at N_q frequencies in the range 1–18 GHz and the resulting electric field is collected around the target on a circular measurement domain S (of radius $R_{mes} = 1.67$ m) at $N_r = 241$ receiver positions. The propagation direction ϕ of the incident wave lies in the (x, y) plane and can be varied ($\phi \in [0, 2\pi]$), N_v views being carried out at varying incidence for each frequency q . The different media are supposed to be linear isotropic and non-magnetic and are characterised by their propagation constant $k(\vec{r})$ such that $k^2(\vec{r}) = k_0^2 = \omega^2 \varepsilon_0 \mu_0$, $\vec{r} = (x, y) \notin \Omega$, where ε_0 and μ_0 represent the dielectric permittivity and the magnetic permeability of vacuum, respectively, or $k^2(\vec{r}) = k_\Omega^2(\vec{r}) = \omega^2 \varepsilon(\vec{r}) \mu_0$, $\vec{r} \in \Omega$, where ε is the complex permittivity ($\varepsilon(\vec{r}) = \varepsilon_0 \varepsilon_r(\vec{r}) + i\sigma(\vec{r})/\omega$) and ε_r and σ represent the relative permittivity and the conductivity of the target, respectively.

The situation is such that a 2D configuration is considered: the TM polarisation case, where the electric field \vec{E} is parallel to the cylinder axis \vec{Oz} , has been the subject of a previous paper [2] published in a

*Corresponding author. Tel.: +33 1 69 85 17 47; Fax: +33 1 69 85 17 65; E-mail: Olivier.Feron@lss.supelec.fr.

special section dedicated to the test of inversion algorithms against experimental data [3]; we consider, herein, the TE polarisation case, where the electric field lies in the (x, y) plane. Let us notice that, in that case, the data consist of the electric field component tangential to the measurement circle.

Modelling is based upon a domain integral representation obtained by applying Green's theorem to the Helmholtz wave equations satisfied by the fields and accounting for continuity and radiation conditions. This leads to two coupled contrast-source integral equations, denoted as the state and observation equations, that express the total electric field \vec{E} inside the domain Ω occupied by the object and the scattered field \vec{E}^{dif} observed on the measurement domain S , respectively:

$$\vec{E}(\vec{r}) = \vec{E}^{inc}(\vec{r}) + \int_{\Omega} \mathcal{G}(\vec{r}, \vec{r}') \vec{J}(\vec{r}') d\vec{r}' + \frac{1}{k_0^2} \vec{\nabla} \vec{\nabla} \cdot \int_{\Omega} \mathcal{G}(\vec{r}, \vec{r}') \vec{J}(\vec{r}') d\vec{r}' \quad \vec{r} \in \Omega \quad (1)$$

$$\vec{E}^{dif}(\vec{r}) = \int_{\Omega} \mathcal{G}(\vec{r}, \vec{r}') \vec{J}(\vec{r}') d\vec{r}' + \frac{1}{k_0^2} \vec{\nabla} \vec{\nabla} \cdot \int_{\Omega} \mathcal{G}(\vec{r}, \vec{r}') \vec{J}(\vec{r}') d\vec{r}' \quad \vec{r} \in S, \quad (2)$$

where $\vec{J}(\vec{r}') = \chi(\vec{r}') \vec{E}(\vec{r}')$ are the induced currents, $\chi(\vec{r}') = k^2(\vec{r}') - k_0^2$ is a contrast function null outside Ω , $\mathcal{G}(\vec{r}, \vec{r}') = \frac{i}{4} H_0^1(k_0 R)$ is the free space Green's function and $R = |\vec{r} - \vec{r}'|$. The contrast function χ characterises the unknown object and the inverse problem then consists in retrieving this function. In a TM configuration [2], these coupled equations become simple and scalar, whereas, in the TE configuration considered herein, the electric field is a two-component vector and the problem is then more involved. It can be noticed that, as the operator $\vec{\nabla} \vec{\nabla}$ acts upon a convolution product, several strategies [4–6] can be used to solve Eqs (10) and (11): i) both of the differential operators can be applied to the Green's function or ii) one can be applied to the latter and the other to the induced currents. The latter strategy is adopted herein. Equation (10) then reads:

$$\vec{E}(\vec{r}) = \vec{E}^{inc}(\vec{r}) + \int_{\Omega} \mathcal{G}(\vec{r}, \vec{r}') \vec{J}(\vec{r}') d\vec{r}' - \frac{1}{k_0^2} \int_{\Omega} \vec{\nabla}' \mathcal{G}(\vec{r}, \vec{r}') \vec{\nabla}' \cdot \vec{J}(\vec{r}') d\vec{r}' \quad \vec{r} \in \Omega, \quad (3)$$

where $\vec{\nabla}'$ means a derivation with respect to the variable \vec{r}' and the observation equation is of the same form.

With in mind the fact that we want to solve the above equations by means of the method of moments, we partition the test domain into elementary square pixels Ω_m of constant complex permittivity. Then, by expressing $\vec{\nabla}' \cdot \vec{J}(\vec{r}')$ as a function of the electric flux $\vec{D} = \varepsilon \vec{E}$, we found that the former vanishes everywhere except at the frontier \mathcal{C} between pixels of different contrasts. By accounting for the continuity of the normal component of \vec{D} across the latter, this reads:

$$-\frac{1}{k_0^2} \vec{\nabla}' \cdot \vec{J}(\vec{r}') = \varepsilon(\vec{r}') \vec{E}(\vec{r}') \cdot \vec{\nabla}' \frac{1}{\varepsilon(\vec{r}')} = \varepsilon(\vec{r}') \vec{E}(\vec{r}') \cdot \vec{n}_{\mathcal{C}} \zeta(\vec{r}') \delta_{\mathcal{C}}(\vec{r}'), \quad (4)$$

where $\vec{n}_{\mathcal{C}}$ is the normal to the contour \mathcal{C} , $\zeta(\vec{r}')$ is the jump of the function $1/\varepsilon(\vec{r}')$ across the latter and $\delta_{\mathcal{C}}$ is the Dirac delta function centred on \mathcal{C} . This means that the second integral in Eq. (3) is reduced to a line integral along the contours of the above-mentioned pixels.

By applying the method of moments with point matching and pulse basis functions H_m , defined as $H_m(\vec{r}) = 1$ if $\vec{r} \in \Omega_m$, $1/2$ if $\vec{r} \in \mathcal{C}_m$ and 0 elsewhere, where Ω_m and \mathcal{C}_m represent the pixel m and its

contour, respectively, we obtain discrete versions of the observation and state equations:

$$\vec{E}(\vec{r}) = \vec{E}^{inc}(\vec{r}) + \mathbf{G}^\Omega \vec{E}(\vec{r}) \quad \vec{r} \in \Omega \quad (5)$$

$$\vec{E}^{dif}(\vec{r}) = \mathbf{G}^S \vec{E}(\vec{r}) \quad \vec{r} \in \mathcal{S}, \quad (6)$$

These two equations are of the same kind as in the TM configuration, but obviously the expressions of the operators \mathbf{G}^Ω and \mathbf{G}^S , that act from Ω onto itself and from Ω onto \mathcal{S} , respectively, are a little bit more intricate and 4 times bigger. Equation (5) (as well as Eq. (6)) can be decomposed into two scalar equations of the form:

$$E_u(\vec{r}) = E_u^{inc}(\vec{r}) + \sum_{m=1}^{N_\Omega} [\chi(\vec{r}_m) G_0^\Omega(\vec{r}, \vec{r}_m) E_u(\vec{r}_m) + G_{ux}^\Omega(\vec{r}, \vec{r}_m) E_x(\vec{r}_m) + G_{uy}^\Omega(\vec{r}, \vec{r}_m) E_y(\vec{r}_m)],$$

$$u = x \text{ or } y, \quad (7)$$

where N_Ω is the number of pixels that partition Ω , \vec{r}_m is the centre of the m^{th} pixel, G_0^Ω results from the first integral in Eq. (3) and is obtained analytically by replacing the square pixel by a disc of same area [7] and G_{vx}^Ω and G_{vy}^Ω result from the second integral in Eq. (3) and correspond to line integrals along the parts of the pixel contour that are perpendicular to x and y , respectively. It can be noticed that the last two terms are obtained by means of fast Fourier transforms, integration being performed analytically along the exact contour of the pixels after a spectral decomposition of the Green's function as in [6]; they are of the form:

$$G_{uv}^\Omega(\vec{r}, \vec{r}_m) = \varepsilon(\vec{r}_m) [\zeta(\vec{r}_m + a\vec{v}) Q_{uv}(\vec{r}, \vec{r}_m + a\vec{v}) - \zeta(\vec{r}_m - a\vec{v}) Q_{uv}(\vec{r}, \vec{r}_m - a\vec{v})],$$

$$u = x \text{ or } y, \quad v = x \text{ or } y, \quad (8)$$

where a is the pixel half-side, \vec{v} is a unitary vector oriented along the x or y axis and Q_{uv} is given by:

$$Q_{uv}(\vec{r}, \vec{r}') = \frac{1}{2\pi} \int_{-\infty}^{+\infty} F_{uv} \frac{\sin(\alpha a)}{2\alpha} e^{i\beta|(\vec{r}-\vec{r}') \cdot \vec{v}|} e^{i\alpha((\vec{r}-\vec{r}_m) \cdot \vec{v})} d\alpha,$$

$$w = x \text{ or } y, \quad w \neq v, \quad \vec{r}' = \vec{r}_m \pm a\vec{v}, \quad \beta = \sqrt{k_0^2 - \alpha^2}, \quad \Im m(\beta) \geq 0,$$

$$F_{uv} = \alpha/\beta \text{ if } u \neq v, \quad F_{vv} = \text{sign}((\vec{r} - \vec{r}') \cdot \vec{v}). \quad (9)$$

It can be noticed (see Eq. (8)) that, through $\zeta(\vec{r}_m \pm a\vec{v}) = 1/\varepsilon(\vec{r}_m \pm 2a\vec{v}) - 1/\varepsilon(\vec{r}_m)$, this model introduces an intrinsic correlation between neighbouring pixels, and also a high level of non-linearity with respect to the contrast function χ ; on one hand the prior information that we want to introduce is precisely based upon such a correlation, but, on the other hand, the latter brings a lot of difficulties into the inversion algorithm implementation, especially with respect to memory requirements, that are not yet solved at the present time. This is the reason why we introduce, in a first step, a bilinearized approximation of the direct model which consists in neglecting these correlation terms. The latter can be expressed, as in the TM case, in terms of contrast and induced currents (or contrast sources):

$$\vec{J}(\vec{r}) = \chi(\vec{r}) \vec{E}^{inc}(\vec{r}) + \chi(\vec{r}) \mathbf{G}_0^\Omega \vec{J}(\vec{r}) \quad \vec{r} \in \Omega \quad (10)$$

$$\vec{E}^{dif}(\vec{r}) = \mathbf{G}_0^S \vec{J}(\vec{r}) \quad \vec{r} \in \mathcal{S}. \quad (11)$$

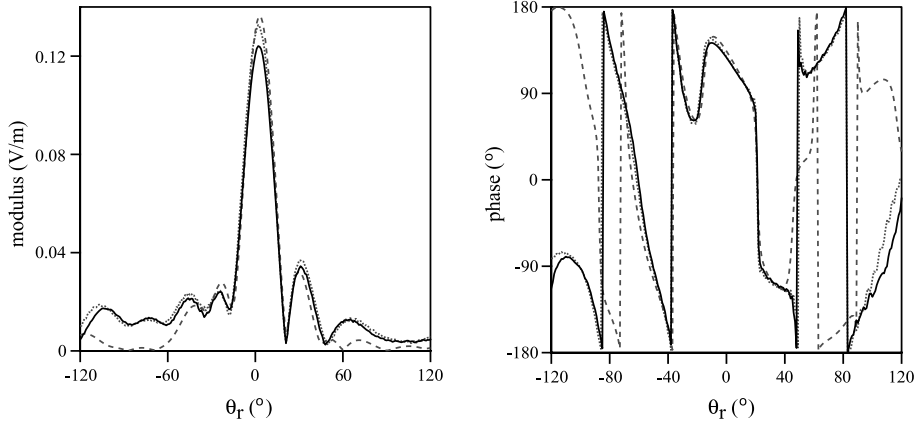


Fig. 1. Modulus (left) and phase (right) of the measured (—) and computed scattered fields obtained by means of the complete (...) and the bilinearized (- -) direct model versus the position of the receiver relative to the direction of illumination ($\theta_r = \phi_r - \phi_e + \pi$).

In order to test the validity of the above considerations, we have compared the results obtained by means of the complete direct model described by Eqs (5) and (6) and those obtained by means of the bilinearized model described by Eqs (10) and (11) to the Institut Fresnel experimental results. Hence, we first solve Eq. (7) for $\vec{E}(\vec{r} = \vec{r}_m)$, $m = 1, \dots, N_\Omega$ (or Eq. (10) for $\vec{J}(\vec{r})$), and then $\vec{E}^{dif}(\vec{r})$, $\vec{r} \in \mathcal{S}$, is obtained directly from the discrete counterpart of Eq. (6) (or of Eq. (11), respectively). Solving Eq. (7) requires the knowledge of the incident field $\vec{E}^{inc}(\vec{r})$ inside Ω . The latter is supposed to be as follows:

$$\vec{E}^{inc}(\vec{r}) = f(\theta) H_0^1(k_0 R) \vec{u}_\theta, \quad (12)$$

where $\vec{R} = \vec{r} - \vec{r}_e = (R, \Phi)$, $\vec{r}_e = (r_e = R_{mes}, \phi_e)$ is the position of the emitting antenna, $\theta = \Phi - \phi_e + \pi$, \vec{u}_θ is a unitary vector such that $\vec{u}_\theta \perp \vec{R}$ and $f(\theta)$ is a directivity factor obtained from the incident field measured on S .

Figure 1 displays the results obtained for the configuration studied in [1], Fig. 9, the latter being chosen for comparison purposes. The target under consideration corresponds to the data set *FoamDielExtTE* in the Institut Fresnel data-base. It is illuminated by an emitting antenna located at $\phi_e = 270^\circ$ and operating at a 8 GHz frequency. The domain Ω is a rectangular area partitioned into 34×25 pixels with side $2a = 3.5$ mm, which corresponds to a discretization step of $\lambda/10.7$, where λ is the wavelength.

It can be concluded that the complete model yields good results, as compared to the experimental ones, which are similar to those obtained in [1] by means of a different model based upon contour integrals, whereas the results obtained by means of the bilinearized model are less good but seem to be satisfactory enough for the inversion task.

2. Inversion algorithm: Prior information and Bayesian approach

Inverse problems in microwave imaging are known to be very ill-posed. Hence a regularization is required prior to their resolution. The latter consists generally in introducing a priori information on the sought solution such as positivity [8], smoothness, or the fact that it is both smoothly varying and piecewise constant [9] or that it contains edges to be preserved [10]. Herein, we introduce a particular

additional information: although the materials that compose the object are not known, their number N_l is supposed to be known and finite. We introduce this prior information, through a Bayesian approach, by modelling the contrast image by a hidden Markov random field. This consists in considering a hidden variable $\mathbf{z}(\vec{r})$ which represents a classification of the contrast image. This hidden variable takes discrete values between 1 and N_l , each value being associated to a given material. Each material will thus be identified by a label n in the image \mathbf{z} and characterised by a mean complex value m_n (associated to its estimated complex permittivity) and a variance ρ_n that allows some fluctuations around the latter and that is considered, herein, as identical for all the labels ($\rho_n = \rho, \forall n = 1, \dots, N_l$).

Let subscripts q and v stand for the frequency and the view, respectively, \mathbf{A} stands for the set that includes all frequencies and views ($\mathbf{A} = \{A_{q,v}\}, q = 1, \dots, N_q, v = 1, \dots, N_v$), except when a subscript does appear where only the latter is of concern, $\vec{\mathbf{A}}$ stands for the set that accounts also for the co-ordinates ($\vec{\mathbf{A}} = \{\mathbf{A}_u\}, u = x, y$) and \mathbf{G}^S and \mathbf{G}^Ω stand for $\mathbf{G}_{0,q,v}^S$ and $\mathbf{G}_{0,q}^\Omega$, respectively.

Let us rewrite the observation and state equations with additive noises $\vec{\mathbf{b}}$ and $\vec{\eta}$, respectively, that account for measurement and model errors. We assume that these noises are Gaussian, white and centred ($\vec{\mathbf{b}} \sim \mathcal{N}(0, \rho_{\vec{\mathbf{b}}} \mathbf{I}_d)$, $\vec{\eta} \sim \mathcal{N}(0, \rho_{\vec{\eta}} \mathbf{I}_d)$) and independent of the frequency and the view. The likelihood function can then be expressed as:

$$p(\vec{\mathbf{E}}^{dif} | \vec{\mathbf{J}}, \rho_{\vec{\mathbf{b}}}) \propto \exp \left\{ -\frac{1}{2\rho_{\vec{\mathbf{b}}}} \sum_{q,v} \|\vec{\mathbf{E}}^{dif} - \mathbf{G}^S \vec{\mathbf{J}}\|_S^2 \right\}. \quad (13)$$

Let us now define a prior conditional probability distribution of the contrast as a Gaussian law: for each pixel \vec{r} of the contrast image, $p(\chi(\vec{r}) | \mathbf{z}(\vec{r}) = n, m_n, \rho) = \mathcal{N}(m_n, \rho)$. The distribution of the entire vector χ , given \mathbf{z} , $\mathbf{m} = \{m_n\}_{n=1, \dots, N_l}$ and ρ , reads then as follows:

$$p(\chi | \mathbf{z}, \mathbf{m}, \rho) = \mathcal{N}(\mathbf{m}_z, \rho \mathbf{I}_d) \propto \exp \left\{ -\frac{1}{2\rho} \|\chi - \mathbf{m}_z\|_\Omega^2 \right\}, \quad (14)$$

with $m_z(\vec{r}) = m_n$ if $z(\vec{r}) = n$.

We focus herein on the joint estimation of the contrast and the induced currents related to the contrast by the state equation (10). Their prior distribution reads as follows:

$$p(\vec{\mathbf{J}}, \chi | \mathbf{z}, \mathbf{m}, \rho) \propto \exp \left\{ -\frac{1}{2\rho_{\vec{\eta}}} \sum_{u,q,v} \|\vec{\mathbf{J}} - \chi_q \vec{\mathbf{E}}^{inc} - \chi_q \mathbf{G}^\Omega \vec{\mathbf{J}}\|_\Omega^2 - \frac{1}{2\rho} \|\chi - \mathbf{m}_z\|_\Omega^2 \right\}, \quad (15)$$

where the first term in the exponential accounts for the state equation and the second term expresses the hidden Markov model of the contrast. Obviously the classification \mathbf{z} and all the parameters m_n and ρ have also to be estimated, as the materials themselves are not known. Prior probability distributions have then to be assigned to these variables. As the materials are supposed to be distributed in compact regions, a local spatial correlation on the pixels of the classification is introduced by modelling \mathbf{z} with a Potts Markov random field:

$$p(\mathbf{z}) \propto \exp \left\{ \sum_{\vec{r} \in \Omega} \sum_{\vec{r}' \in \mathcal{V}(\vec{r})} \delta(\mathbf{z}(\vec{r}) - \mathbf{z}(\vec{r}')) \right\}, \quad (16)$$

where δ is the Kronecker function and $\mathcal{V}(\vec{r})$ is the set of the four nearest neighbours of the pixel \vec{r} . The prior probability distributions of the parameters m_n and ρ are chosen to be in the so-called ‘‘conjugate prior’’ family in order to render their estimation easier. In a totally unsupervised estimation framework, the parameters $\rho_{\vec{r}}$ and $\rho_{\vec{r}}$ have also to be estimated; however, herein, these two parameters are manually fixed in order to control the respective weights of the likelihood Eq. (13) and of the two terms of the prior Eq. (15).

We can now define a joint prior distribution $p(\vec{\mathbf{J}}, \chi, \mathbf{z}, \mathbf{m}, \rho)$ of all the unknowns that takes into account the state equation (10) and all the information introduced earlier. By using the Bayes formula, the *a posteriori* distribution of all the unknowns, given the scattered field data, can be expressed as:

$$p(\vec{\mathbf{J}}, \chi, \mathbf{z}, \mathbf{m}, \rho \mid \vec{\mathbf{E}}^{dif}) \propto p(\vec{\mathbf{E}}^{dif} \mid \vec{\mathbf{J}}, \rho_{\vec{r}}) p(\vec{\mathbf{J}}, \chi \mid \mathbf{z}, \mathbf{m}, \rho) p(\mathbf{z}) p(\mathbf{m}, \rho) \quad (17)$$

This posterior distribution represents all the information we have on the unknowns that accounts for the *a priori* knowledge and the data. The Bayesian approach consists then in using this posterior distribution to define an estimator for the unknowns. We propose to estimate the posterior mean by means of a Gibbs sampling algorithm. This consists in splitting the set of variables into subsets and alternately sample these subsets from their conditional probability distributions. Herein, we partition the set of variables into three subsets: $\vec{\mathbf{J}}$, (χ, \mathbf{z}) and (\mathbf{m}, ρ) . The Gibbs sampling algorithm then reads: given an initialisation $\vec{\mathbf{J}}^{(0)}$, $\chi^{(0)}$ and $\mathbf{z}^{(0)}$,

repeat

1. sample $(\mathbf{m}^{(n)}, \rho^{(n)}) \sim p(\mathbf{m}, \rho \mid \vec{\mathbf{J}}^{(n-1)}, \chi^{(n-1)}, \mathbf{z}^{(n-1)}, \vec{\mathbf{E}}^{dif})$
 2. sample $(\chi^{(n)}, \mathbf{z}^{(n)}) \sim p(\chi, \mathbf{z} \mid \vec{\mathbf{J}}^{(n-1)}, \mathbf{m}^{(n)}, \rho^{(n)}, \vec{\mathbf{E}}^{dif})$
 3. sample $\vec{\mathbf{J}}^{(n)} \sim p(\vec{\mathbf{J}} \mid \chi^{(n)}, \mathbf{z}^{(n)}, \mathbf{m}^{(n)}, \rho^{(n)}, \vec{\mathbf{E}}^{dif})$
-

Because the hyper-parameters (\mathbf{m}, ρ) are chosen as the conjugate priors, the sampling of $p(\mathbf{m}, \rho \mid \vec{\mathbf{J}}, \chi, \mathbf{z}, \vec{\mathbf{E}}^{dif})$ is easy and comes down to sample $\rho^{(n)}$ from an Inverse Gamma law and to sample the means $m^{(n)}$ from Gaussian distributions.

Applying the product rule leads to:

$$\begin{aligned} p(\chi, \mathbf{z} \mid \vec{\mathbf{J}}, \mathbf{m}, \rho, \vec{\mathbf{E}}^{dif}) &= p(\chi \mid \mathbf{z}, \vec{\mathbf{J}}, \mathbf{m}, \rho, \vec{\mathbf{E}}^{dif}) p(\mathbf{z} \mid \vec{\mathbf{J}}, \mathbf{m}, \rho, \vec{\mathbf{E}}^{dif}) \\ &= p(\chi \mid \mathbf{z}, \vec{\mathbf{J}}, \mathbf{m}, \rho) p(\mathbf{z} \mid \vec{\mathbf{J}}, \mathbf{m}, \rho) \end{aligned} \quad (18)$$

Thus, a joint sample $(\chi^{(n)}, \mathbf{z}^{(n)})$ is obtained by first sampling $\mathbf{z}^{(n)}$ from $p(\mathbf{z} \mid \vec{\mathbf{J}}, \mathbf{m}, \rho)$ and then sampling $\chi^{(n)}$ from $p(\chi \mid \mathbf{z}, \vec{\mathbf{J}}, \mathbf{m}, \rho)$. The distribution $p(\mathbf{z} \mid \vec{\mathbf{J}}, \mathbf{m}, \rho)$ is obtained by using the Bayes formula:

$$p(\mathbf{z} \mid \vec{\mathbf{J}}, \mathbf{m}, \rho) \propto p(\vec{\mathbf{J}} \mid \mathbf{z}, \mathbf{m}, \rho) p(\mathbf{z}), \quad (19)$$

where $p(\mathbf{z})$ is the Potts prior distribution of \mathbf{z} , and the expression of $p(\vec{\mathbf{J}} \mid \mathbf{z}, \mathbf{m}, \rho)$ can be obtained by integrating $p(\vec{\mathbf{J}}, \chi \mid \mathbf{z}, \mathbf{m}, \rho)$ with respect to χ . As a result of this integration, $p(\vec{\mathbf{J}} \mid \mathbf{z}, \mathbf{m}, \rho)$ is a separable function of the pixels with respect to \mathbf{z} . Therefore, the conditional distribution $p(\mathbf{z} \mid \vec{\mathbf{J}}, \mathbf{m}, \rho)$ is a Markov random field with a neighbouring system of four pixels, as its prior distribution. The sampling of this kind of distribution is easy [2].

Concerning the sampling of χ , the conditional distribution $p(\chi \mid \mathbf{z}, \vec{\mathbf{J}}, \mathbf{m}, \rho)$ is directly obtained from the joint prior distribution $p(\chi, \vec{\mathbf{J}} \mid \mathbf{z}, \mathbf{m}, \rho)$ and the product rule. By using the Bayes formula, we get:

$$p(\vec{\mathbf{J}} \mid \chi, \mathbf{z}, \mathbf{m}, \rho, \vec{\mathbf{E}}^{dif}) \propto p(\vec{\mathbf{E}}^{dif} \mid \vec{\mathbf{J}}) p(\vec{\mathbf{J}} \mid \chi, \mathbf{z}, \mathbf{m}, \rho) \quad (20)$$

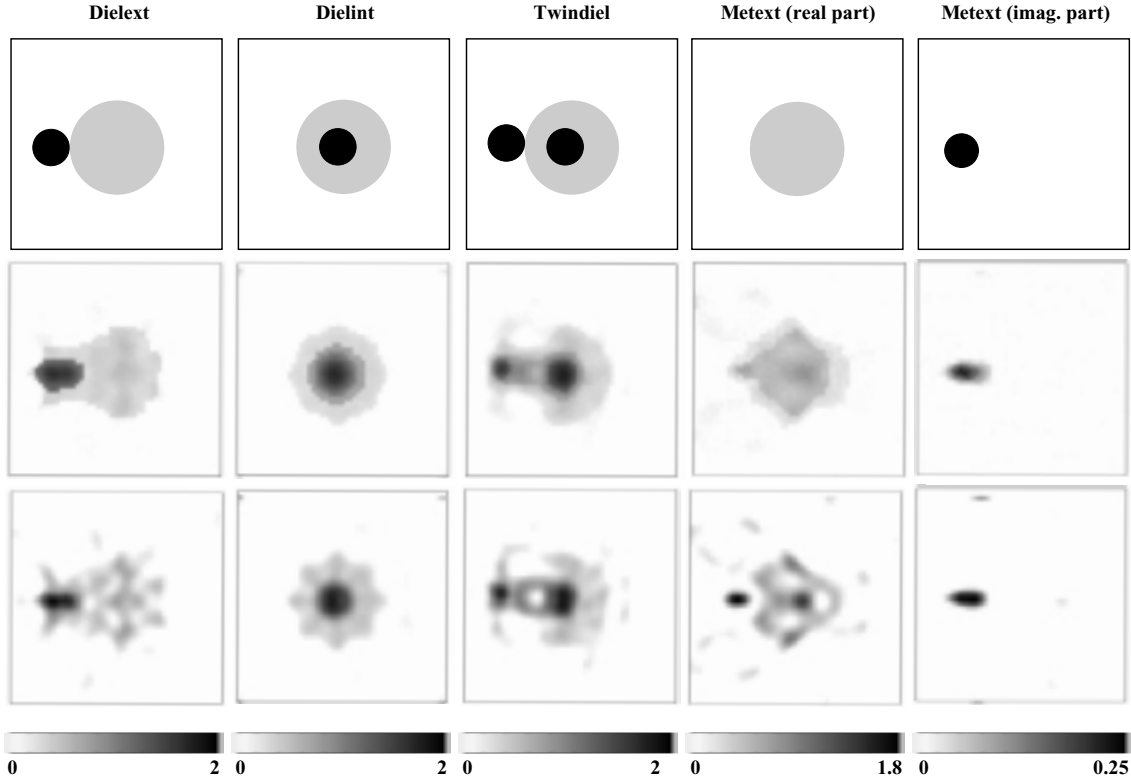


Fig. 2. The true contrast (up) and the contrast retrieved by means of the proposed method (middle) and by means of the CSI method (down) for the four targets of the Institut Fresnel database (Dielect: 1st column, Dielint: 2nd column, Twindiel: 3rd column and Metext: 4th and 5th columns). Both the real and imaginary part of the contrast are displayed for the object Metext, whereas only the real part is displayed for the three other targets.

$$\propto \exp \left\{ - \sum_{u,q,v} \left[\frac{1}{2\rho_b} \|\vec{\mathbf{E}}^{dif} - \mathbf{G}^S \vec{\mathbf{J}}\|_S^2 + \frac{1}{2\rho_{\vec{\eta}}} \|\vec{\mathbf{J}} - \chi_q \vec{\mathbf{E}}^{inc} - \chi_q \mathbf{G}^\Omega \vec{\mathbf{J}}\|_\Omega^2 \right] \right\}.$$

This conditional distribution is in fact Gaussian with a non-diagonal covariance matrix. However, a sample of this distribution can be generated by a maximization technique [2].

3. Results

The above method has been applied to the reconstruction of the four targets (denoted as Dielect, Dielint, Twindiel and Metext, respectively) considered in the *Institut Fresnel* database, which are composed of different dielectric and metallic cylinders (see [1] for a description of their basic features). The results are displayed in Fig. 2. They are compared to those obtained with the contrast source inversion method (CSI) [8]. It can be noticed that only a part of the available data has been used, i.e., four frequencies (3, 5, 7 and 9 GHz), 61 measurement points (each 4°) and 8 (Dielect and Dielint) or 9 (Twindiel and Metext) views around the object. The test domain is a 17.85 cm sided square divided into 51 × 51 pixels with side 3.5 mm. As a general rule our method provides good results concerning the shape reconstruction, the localisation and the estimated values of the contrast for the different materials. As expected, the retrieved

objects are composed of quasi-homogeneous regions. Except for the target Twindiel, the results are comparable to those obtained in the TM case [2]: they are slightly less good than in the latter case, which is not surprising as i) less data are used and ii) the contribution of the discontinuities at the frontiers of the different materials is neglected. This latter point is probably at the origin of the poor results obtained for target Twindiel as the latter presents a complex geometry that is favourable to the enhancement of the effect of the non-linearities linked to the discontinuities. Finally, the contribution of the prior information that we have introduced can be estimated by noticing that the results are much better than those obtained by means of the CSI method.

4. Conclusion

In this paper we present a new approach of inversion in a TE configuration. We propose a solution in order to introduce a particular prior information: the object is composed of a known finite number of different materials distributed in compact regions. First, we have developed an approximated direct model which is bilinearized with respect to the induced currents and to the contrast function. Then, we have implemented an appropriate Gibbs sampling algorithm that takes into account the property of bilinearity and the prior information. The results obtained by means of this approach show its effectiveness. However, better results can be expected by considering the exact direct model; the inverse problem has then to be reformulated with the total field and the contrast as unknowns.

References

- [1] J.-M. Geffrin, P. Sabouroux and C. Eyraud, Free space experimental scattering database continuation: experimental set-up and measurement precision, *Inverse Problems* **21** (2005), S117–S130.
- [2] O. Féron, B. Duchêne and A. Mohammad-Djafari, Microwave imaging of inhomogeneous objects made of a finite number of dielectric and conductive materials from experimental data, *Inverse Problems* **21** (2005), S95–S115.
- [3] K. Belkebir and M. Saillard, Special section on testing inversion algorithms against experimental data: inhomogeneous targets. Guest Editors' introduction, *Inverse Problems* **21** (2005), S1–S4.
- [4] D.E. Livesay and K.M. Chen, *Electromagnetic fields induced inside arbitrarily shaped biological bodies*, IEEE Trans. Microwave Theory Tech. MTT-22, 1974, 1273–1280.
- [5] S.C. Hill, C.H. Durney and D.A. Christensen, Numerical solutions of low-frequency TE fields in arbitrarily shaped inhomogeneous lossy dielectric cylinders, *Radio Sci* **18** (1983), 328–336.
- [6] N. Joachimowicz and C. Pichot, *Comparison of three integral formulations for the 2-D TE scattering problem*, IEEE Trans. Microwave Theory Tech. MTT-38, 1990, 178–185.
- [7] J.H. Richmond, *TE-wave scattering by a dielectric cylinder of arbitrary cross-section shape*, IEEE Trans. Antennas Propagat. AP-14, 1966, 460–464.
- [8] P.M. van den Berg and R.E. Kleinman, A contrast source inversion method, *Inverse Problems* **13** (1997), 1607–1620.
- [9] P.M. van den Berg and R.E. Kleinman, A total variation enhanced modified gradient algorithm for profile reconstruction, *Inverse Problems* **11** (1995), L5–L10.
- [10] P. Charbonnier, L. Blanc-Féraud, G. Aubert and M. Barlaud, *Deterministic edge-preserving regularization in computed imaging*, IEEE Trans. Image Process. IP-6, 1997, 298–311.